Gray, L. H., Conger, A. D., Ebert, M., Hornsey, S., & Scott, O. C. (1953) *Br. J. Radiol. 26*, 638–648.
Grunberg, S. M., & Haseltine, W. A. (1980) *Proc. Natl. Acad. Sci. U.S.A. 77*, 6546–6550.
Hutterman, J., Kohnlein, W., & Teoule, R., Eds. (1978) *Effects of Ionizing Radiation on DNA: Physical, Chemical and Biological Aspects*, p 374, Springer-Verlag, New York.
Ide, H., Kow, Y. W., & Wallace, S. S. (1985) *Nucleic Acids Res. 13*, 8035–8052.
Iida, S., & Hayatsu, H. (1970) *Biochim. Biophys. Acta 213*, 1–13.
Iida, S., & Hayatsu, H. (1971) *Biochim. Biophys. Acta 240*, 370–375.
Mottram, J. C. (1936) *Br. J. Radiol. 9*, 606–614.
Read, J. (1952) *Br. J. Radiol. 25*, 89–99.
Rouet, P., & Essigmann, J. M. (1985) *Cancer Res. 45*, 6113–6118.
Scholes, G. (1978) in *Effects of Ionizing Radiation on DNA: Physical, Chemical and Biological Aspects* (Hutterman, J., Kohnlein, W., & Teoule, R., Eds.) pp 153–170, Springer-Verlag, New York.
Teebor, G. W., Frenkel, K., & Goldstein, M. S. (1982) *Adv. Enzyme Regul. 20*, 39–54.
Teebor, G. W., Frenkel, K., & Golstein, M. S. (1984) *Proc. Natl. Acad. Sci. U.S.A. 81*, 318–321.
Teoule, R., Bonicel, A., Bert, C., & Fouque, B. (1978) *J. Am. Chem. Soc. 100*, 6749–6750.
Ward, J. F. (1981) *J. Chem. Educ. 58*, 135–139.

Nucleotide Sequence Binding Preferences of Nogalamycin Investigated by DNase I Footprinting†

Keith R. Fox* and Michael J. Waring

Department of Pharmacology, Medical School, University of Cambridge, Cambridge CB2 2QD, U.K.

Received December 30, 1985; Revised Manuscript Received March 17, 1986

ABSTRACT: Four DNA restriction fragments, designated *tyrT*, *pTyr2*, *pUC13*, and *Xbs1*, have been used as substrates for footprinting studies with DNase I in the presence of the anthracycline antibiotic nogalamycin. With each fragment a distinct pattern of antibiotic-protected binding sites is observed, but no concensus sequence emerges from the data. All sites are located in regions of alternating purine–pyrimidine sequence, most commonly associated with the dinucleotide steps TpG (CpA) and GpT (ApC), suggesting that the preferred binding sites may contain all four nucleotides and/or that peculiarities of the dynamics of DNA conformation at alternating sequences may be critical for nogalamycin binding. Some concentration dependence of footprinting patterns is evident, in contrast to previous studies with a variety of sequence-specific ligands. Enhanced susceptibility to attack by DNase I is commonly observed at sequences flanking strong antibiotic-binding sites. Nogalamycin selectively inhibits cleavage of DNA at certain guanine-containing sequences by the G-specific photosensitized reaction with methylene blue. Comparison of these effects with its action on the G-specific reaction with dimethyl sulfate suggests that the amino sugar moiety of nogalamycin may be preferentially located in the minor helical groove at some binding sites but in the major groove at others.

Nogalamycin (Figure 1) is an anthracycline antibiotic that has been reported to show activity against experimental tumors both in vivo and in vitro (Bhuyan & Deitz, 1965; Bhuyan & Reusser, 1970; Brown, 1983). Most anthracyclines bear a sugar substituent at position 7 on the nonaromatic A ring of the chromophore; others (such as iremycin) have one on the opposite side of the A ring at position 10 (Arcamone, 1981; Ihn et al., 1980). The structure of nogalamycin is unique insofar as it bears bulky sugar residues at both ends of its anthracycline chromophore (Arora, 1983). Nevertheless, it retains the property of binding strongly to double-helical DNA by the well-investigated mechanism of intercalation (Kersten et al., 1966; Waring, 1970; Plumbridge & Brown, 1979). The current model proposed for its interaction with DNA involves positioning of the two sugar moieties in each of the helical grooves, with the chromophore "spearing" the stack of base pairs (Arora, 1983; Collier et al., 1984; Fox & Waring, 1984a). While this model is sterically feasible, it poses considerable dynamic problems since the minimum width of the antibiotic is 1.2 nm, whereas it is not possible to open a potential DNA intercalation site beyond about 1.0 nm (Collier et al., 1984). We have previously shown that an important consequence of this limitation is apparent in the kinetics of antibiotic binding, which are markedly dependent upon the precise nucleotide sequence. The antibiotic binds fastest to those sequences that are easier to disrupt (Fox & Waring, 1984) yet dissociates most slowly from the more stable regions (Fox et al., 1985).

In all these respects, nogalamycin behaves very differently from such simple anthracyclines as daunomycin. On the basis of our kinetic findings, we predicted that nogalamycin might display some peculiar sequence preferences, binding best to those regions of DNA that are most easily disrupted (melted) yet that can be most strongly stabilized by the presence of the antibiotic. Previous investigations aimed at detecting possible base sequence selectivity in the binding of this antibiotic to

† This work was supported by grants from the Cancer Research Campaign, The Royal Society, and the Medical Research Council.

0006-2960/86/0425-4349$01.50/0

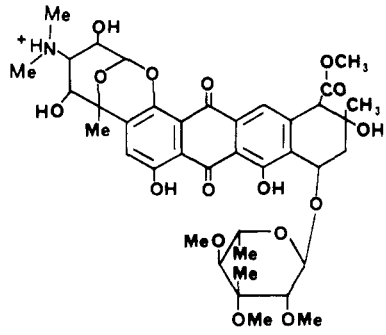

FIGURE 1: Structure of nogalamycin.

DNA have yielded conflicting results. Some have suggested an affinity for AT-rich regions (Bhuyan & Smith, 1965) and some for G and C (Kersten et al., 1966), whereas others have reported that it displays little or no sequence selectivity (Chowdhury et al., 1978).

In this paper we have employed the technique of DNase I footprinting to locate the precise binding sites for nogalamycin on four DNA fragments of defined sequence. Footprinting is a method that combines the enzymatic (or chemical) cleavage of DNA with analysis of the products by sequencing gels. Sites to which the antibiotic is bound are protected from cleavage and are visualized at single-bond resolution as gaps in the autoradiograph of a denaturing polyacrylamide gel, revealing the position and length of each ligand binding site. The general applicability of this technique is well established: it has previously been used with considerable success to investigate the DNA sequence selectivity of actinomycin D, distamycin, chromomycin, and quinoxaline antibiotics (Lane et al., 1983; Van Dyke et al., 1982; Van Dyke & Dervan, 1983; Fox & Waring, 1984b; Low et al., 1984a,b).

Materials and Methods

Antibiotics and Enzymes. Nogalamycin was a gift from Dr. P. F. Wiley, the Upjohn Co., Kalamazoo, MI. Daunomycin was a gift from Dr. F. Arcamone, Farmitalia, Milan, Italy. Iremycin was obtained from Dr. H. Fritzsche, Central Institute for Microbiology and Experimental Therapy, Academy of Sciences of the GDR Jena. Stock solutions of each antibiotic were prepared by direct weighing and dissolved in 10 mM tris(hydroxymethyl)aminomethane hydrochloride (Tris-HCl), pH 7.5, containing 10 mM NaCl Deoxyribonuclease I (DNase I) was obtained from Sigma and prepared as a 7200 units/mL stock solution in 0.15 M NaCl containing 1 mM $MgCl_2$. This was stored at −20 °C and diluted to working concentrations immediately before use.

DNA Substrates. The 160-base-pair *tyrT* fragment was isolated and labeled as previously described (Drew & Travers, 1984). Incubation with reverse transcriptase, dGTP, and [α-32p]dCTP led to selective labeling of the 3′ end of the top strand (Figure 3) whereas incubation with dTTP and [α-32p]dATP led to selective labeling of the 3′ end of the bottom strand. Bands in the *tyrT* digestion pattern were assigned by comparing the pattern in control lanes with that previously described (Low et al., 1984a,b; Drew & Travers, 1984).

The 166-base-pair *pTyr*2 fragment (Figure 4b) was cut from plasmid pMLB1048 between the unique *Eco*RI and *Bst*EII sites and was a gift from Dr. C. M. L. Low. The *Bst*EII end (top strand) was selectively labeled with dGTP and [α-^{32}P]-dTTP while the *Eco*RI end (bottom strand) was labeled with dTTP and [α-^{32}P]dATP.

The 49-base-pair *pUC13* multiple cloning site fragment (Figure 5b) was purchased from P-L Biochemicals and used without further purification. The *Eco*RI site (top strand) was labeled at its 3′ end eith dATP and [α-^{32}P]dTTP while the *Hin*dIII site (bottom strand) was labeled with dATP, dGTP, and [α-^{32}P]dCTP.

The 119-base-pair *Xbs*1 fragment was cut from plasmid pXbs1, which contains a single repeating unit of *Xenopus borealis* somatic 5S DNA in plasmid pBR322 (Peterson et al., 1980) between the unique *Hin*dIII site and the first *Ava*I site on the inserted DNA. The fragment was labeled as previously described (Fox & Howarth, 1985).

DNase I Footprinting. Samples (3 μL) of the labeled DNA fragment (9 pmol in base pairs) were incubated with 5 μL of antibiotic solution at 37 °C for 30 min, sufficient to ensure an equilibrium distribution of the ligand (Fox & Waring, 1986). These were then digested with 2 μL of DNase I dissolved in 20 mM NaCl, 2 mM $MgCl_2$, and 2 mM $MnCl_2$ at a final enzyme concentration of 0.01 unit/mL. Aliquots (3 μL) were removed from the mixture after 1, 5, and 30 min, and the reaction was stopped by adding 2.5 μL of 80% formamide containing 0.1% bromophenol blue, 10 mM ethylenediaminetetraacetic acid (EDTA), and 1 mM NaOH. Samples were heated at 100 °C for at least 3 min prior to electrophoresis.

Reaction with Methylene Blue. Exposure of DNA to methylene blue and visible light has been shown to cause guanine-specific modification, and subsequent treatment with piperidine leads to chain cleavage at the modified guanine residues (Friedmann & Brown, 1978). Typically, the reaction was performed by first incubating the DNA (5 pmol in base pairs) with an appropriate antibiotic solution at 37 °C for 30 min. The mixture was then placed on ice, and an equal volume of 0.2% (w/v) methylene blue was added. This was placed in an Eppendorf tube with the cap open, 10 cm from a 60-W bulb. After 15-min illumination, the DNA was precipitated with ethanol and cleaved with 1 M piperidine at 90 °C. The samples were the lyophilized and taken up in 80% formamide.

Gel Electrophoresis. The products of *tyrT*, *pTyr*2, and *Xbs1* digestion were analyzed on 0.3-mm 8% (w/v) polyacrylamide gels containing 7 M urea and Tris–borate–EDTA buffer, pH 8.3. For the shorter *pUC*13 DNA, the products were resolved on a 12% polyacrylamide gel. After 2-h electrophoresis at 1500 V, the gel was soaked in 10% acetic acid for 10 min, transferred to Whatman 3MM paper, dried under vacuum at 80 °C, and subjected to autoradiography at −70 °C with an intensifying screen.

Densitometry. Autoradiographs were scanned on a Joyce-Loebl microdensitometer to produce profiles from which the relative intensity of each band was measured. The data are expressed as fractional cleavage $f = A_i/A_t$ as previously described (Low et al., 1984a,b; Fox & Waring, 1984b), where A_i is the area under band i and A_t is the sum of the intensity under all bands in any gel lane. When different digestion patterns were compared, care was taken to ensure that the extent of digestion was similar and limited to 20–40% of the starting material so as to minimize the incidence of multiple cuts in any strand, thereby ensuring that cleavage at any site is dependent solely on the concentration of the particular site and is independent of the ligand binding kinetics (Goodisman & Dabrowiak, 1985). Data from this analysis are presented in the form $\ln f_{\text{antibiotic}} - \ln f_{\text{control}}$, representing the differential cleavage at each bond relative to that in the control. The results are displayed on a logarithmic scale for the sake of convenience so that positive values indicate enhanced cleavage whereas negative values indicate blockage.

Results

Typical DNase I digestion patterns for the 160-base-pair

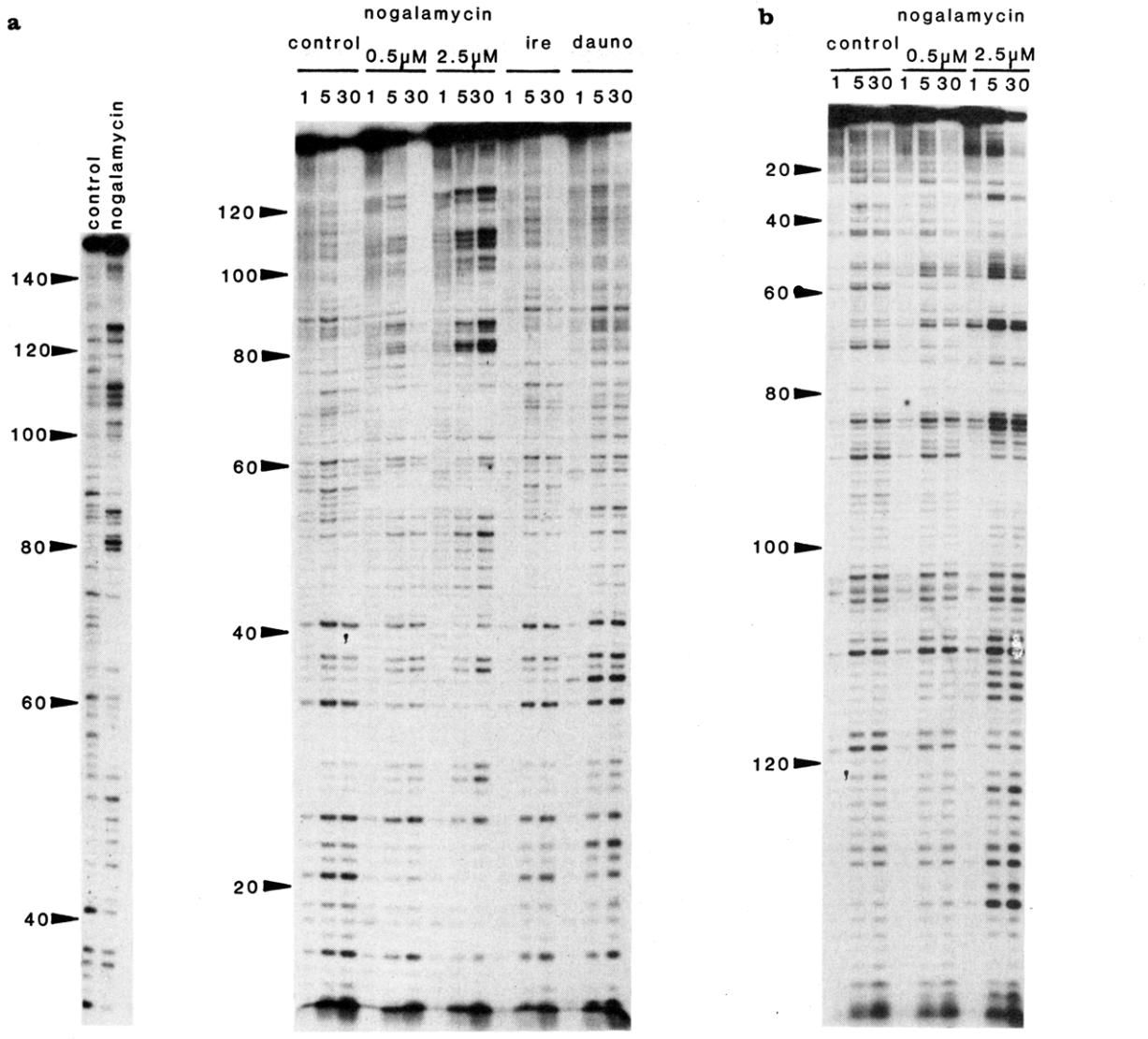

FIGURE 2: DNase I footprinting of nogalamycin (0.5 and 2.5 μM), iremycin (ire, 5 μM), and daunomycin (dauno, 5 μM) on the 160-base-pair *tyrT* DNA fragment whose sequence is shown in Figure 3. Time in minutes (1, 5, and 30) after the addition of enzyme is shown at the top of each gel lane. (a) DNA labeled at the 3′ end of the bottom strand. The two tracks on the far left represent an overrun of the control and 2.5 μM nogalamycin samples removed 5 min after the addition of the enzyme, to provide better separation of the longer fragments. (b) DNA labeled at the 3′ end of the top strand.

tyrT fragment in the presence of low concentrations of nogalamycin are displayed in panels a and b of Figure 2 for the labeled bottom and top strands, respectively. Each gel lane contains about 100 bands that are satisfactorily resolved; these were analyzed as described under Materials and Methods, giving rise to the differential cleavage plot shown in Figure 3. It is immediately apparent that the cleavage pattern in the presence of the antibiotic is substantially different from that of the DNA alone. In the presence of 2.5 μM nogalamycin, six sites protected by the antibiotic can easily be discerned, located near positions 20, 35, 57, 69, 91, 117, affecting both strands. At each site the block is staggered across the two strands by about three bonds toward the 3′ end, as previously observed for DNase I footprinting with other antibiotics (Low et al., 1984a,b; Fox & Waring, 1984b), presumably because DNase I cuts by binding to phosphate groups that lie in close proximity across the double-helical minor groove. The minimum protected region at each site appears to be four or five base pairs. It is also evident that the rate of cleavage at certain bonds is enhanced relative to the control. This is especially noticeable around positions 30, 50, 81, 110, and 127, where the internucleotide linkages are poorly cut in the absence of the antibiotic. Enhanced cutting presumably results from conformational changes in the DNA induced by the binding of the ligand to adjacent sites. Similar enhancement of DNase I cleavage has previously been observed with other sequence-selective ligands (Low et al., 1984a,b; Fox & Waring, 1984b), and the origin of the effect will be considered further under Discussion.

One noteworthy feature is that the pattern of cleavage varies with the antibiotic concentration, in contrast to the situation observed in earlier footprinting studies with a variety of ligands. At 37 °C, no protection is observed below 0.5 μM nogalamycin and the cleavage pattern remains essentially unchanged up to 5–10 μM ligand. However, at higher concentrations the protected regions become longer until in the presence of 50 μM antibiotic the only bands visible result from cutting around positions 80 and 130. This graded response may well reflect a peculiarity of nogalamycin to the effect that it lacks any absolute sequence preference but can bind to many types of sequences with different affinities. It is also worth noting that very low concentrations of nogalamycin are required to produce a distinct footprinting pattern. This must result from very tight binding between the antibiotic and DNA.

Also shown in Figure 2a are footprinting patterns determined with the simpler anthracycline antibiotics iremycin and

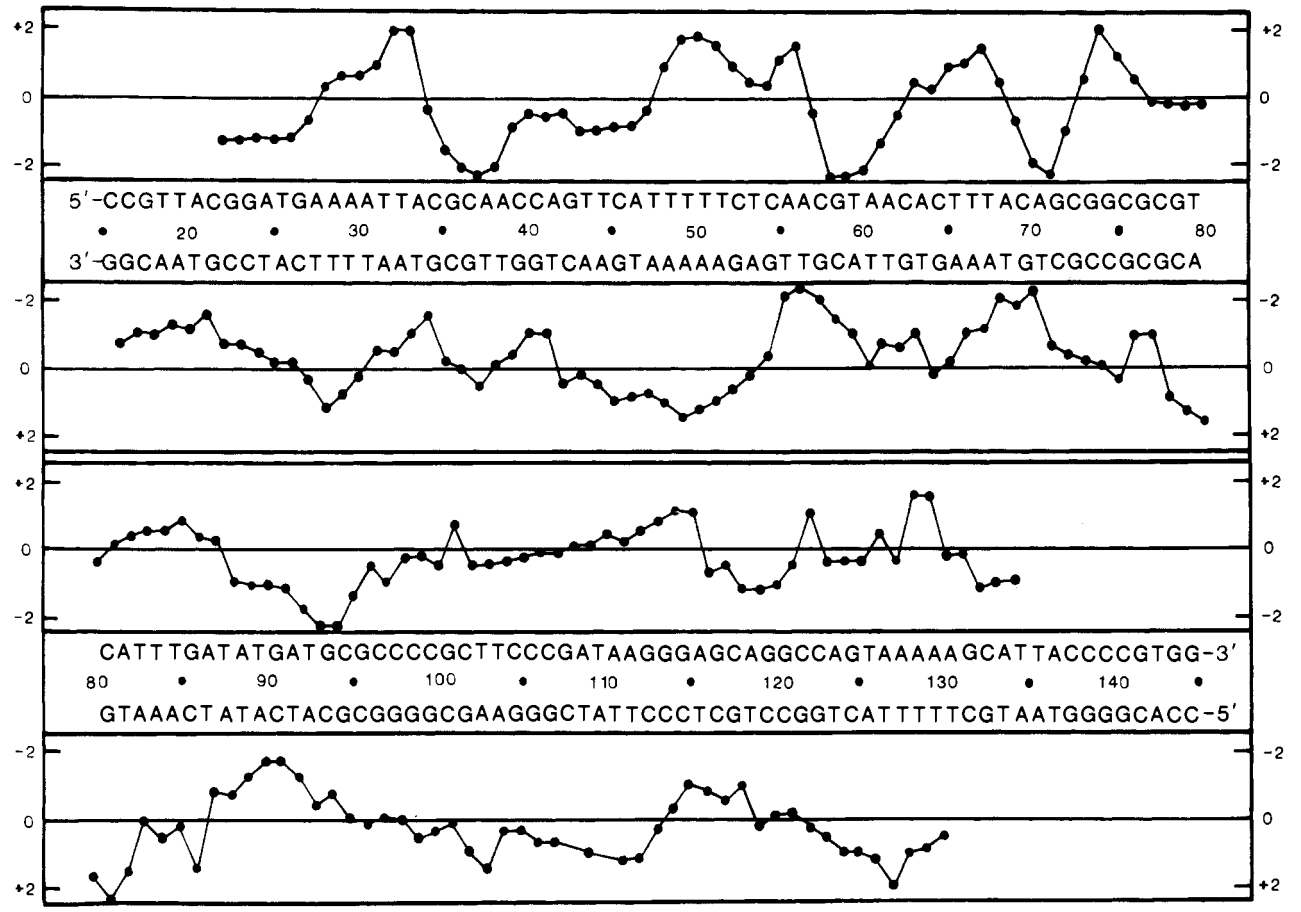

FIGURE 3: Differential cleavage plot for nogalamycin-induced differences in susceptibility of *tyrT* DNA to DNase I cleavage. Vertical scales are in units of $\ln f_a - \ln f_c$, where f_a is the fractional cleavage at any bond in the presence of the antibiotic (2.5 μM) and f_c is the fractional cleavage of the same bond in the control. Positive values indicate enhancement and negative values blockage.

daunomycin. Iremycin at 5 μM has almost no effect on the cleavage pattern. Although daunomycin does not produce distinct gaps in the cutting pattern, characteristic of sequency-selective binding, it does affect the relative intensity of certain bands. For instance, witness the changes in relative band intensity between positions 34 and 41, especially the remarkable enhancement at position 36. Clearly, daunomycin must affect the DNA structure in some subtle way, but the changes it produces are very different from those caused by nogalamycin binding. At higher concentrations (or lower temperatures) daunomycin produces more definite changes in the cleavage pattern, but again there are no clear gaps (results not shown).

Close inspection of the six regions protected by nogalamycin does not reveal any obvious concensus sequence suggestive of simple sequence selectivity. It seems likely that the antibiotic actually recognizes certain conformational and/or dynamic features of the DNA, rather than any particular nucleotide sequence. In order to clarify the situation further, experiments were performed with three other DNA fragments of differing sequence.

A typical DNase I digestion pattern of *pTyr*2 DNA, labeled at the 3′ end of the bottom strand, with and without nogalamycin is displayed in Figure 4a. A differential cleavage plot calculated from the data for both strands is shown in Figure 4b. Once again, regions of enhancement as well as blockage are readily apparent. In this DNA fragment, which has a more "random" sequence than *tyrT* DNA, the blockages seem to extend over much longer tracts of nucleotides, perhaps because of overlapping or clustering of potential antibiotic binding sites. Major protected regions are visible (Figure 4a) around positions 34–46, 76–80, and 84–92 with a large enhancement around position 60. While there is no sequence common to these protected regions, they are each located at positions of alternating purines and pyrimidines, although it is noteworthy that the effects are often a good deal more marked on the "bottom" strand compared to the "top" strand (Figure 4b).

Figure 5a displays the DNase I digestion pattern of the *pUC*13 multiple-cloning fragment, labeled at the 3′ end of the top strand, in the presence and absence of nogalamycin. Only one clear site of blockage is revealed, located around position 14. The results for both strands are presented in the form of a differential cleavage plot in Figure 5b. The only well-protected region on the labeled bottom strand lies around bond number 10 and is not properly resolved; shorter fragments were lost off the end of the gel. What is peculiar about the sequence around this strong nogalamycin binding site? Of the 10 possible dinucleotide pairs, the only one unique to this region is the step CpA (or TpG), which occurs at positions 11 and 13. While it is tempting to speculate that this dinucleotide constitutes the preferred nogalamycin binding site, it may not be the only explanation since this region contains the only stretch of alternating purines and pyrimidines in the fragment.

In additional DNase I footprinting experiments with the *Xbs*1 fragment (data not presented), nogalamycin again produced a pattern of blockages and enhancements, although the protected regions were not so well-defined. The best resolved binding site apparent on both strands was found to be centered around position 68 in the sequence TACACGC, another run of alternating purines and pyrimidines.

In a further attempt to define the nature of nogalamycin binding sites, we examined the effect of this ligand on the

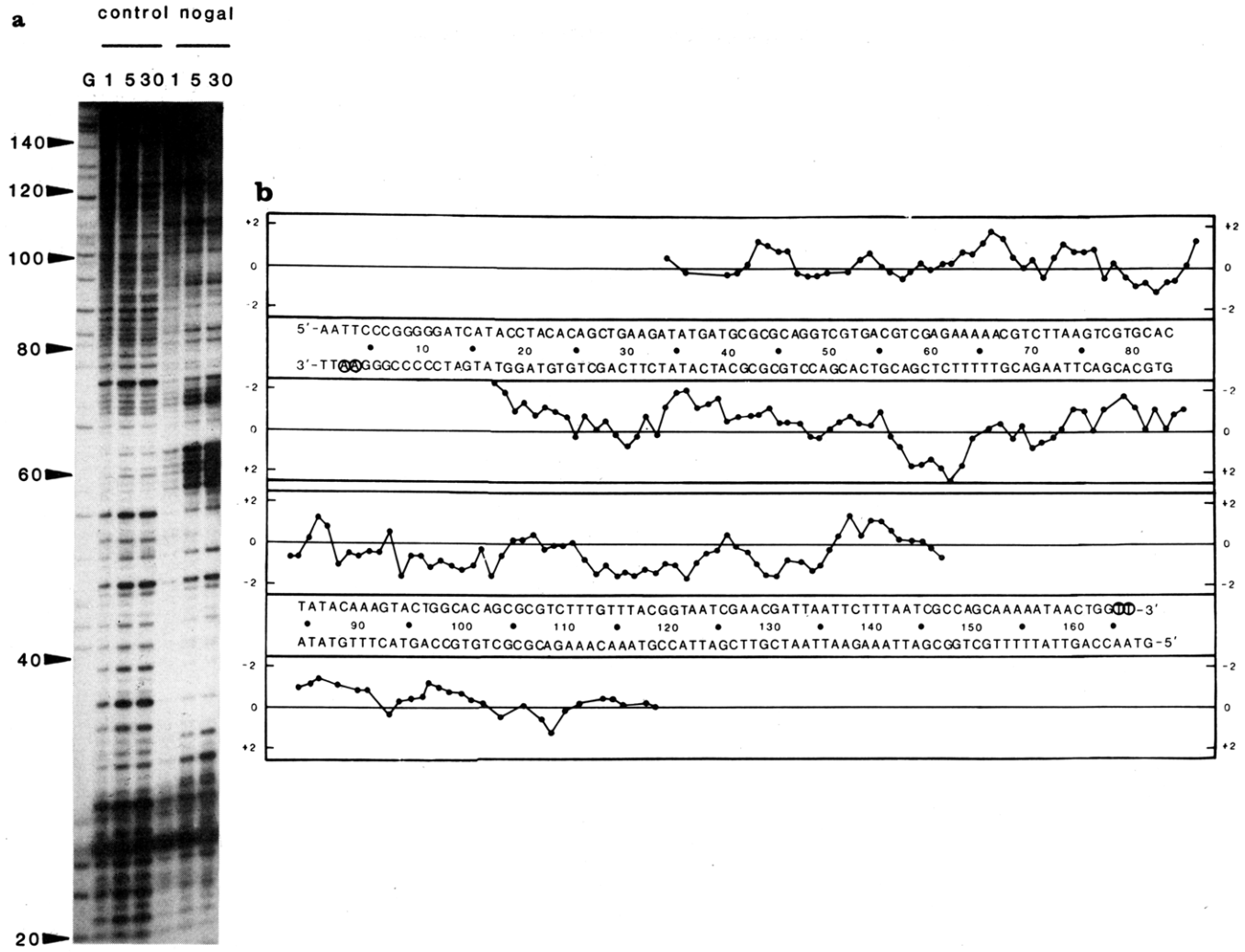

FIGURE 4: (a) DNase I footprinting of nogalamycin (2.5 μM) on *pTyr2* DNA (bottom strand) whose sequence is shown in (b). Time in minutes after the addition of enzyme is shown at the top of each gel lane. The track labeled "G" is a dimethyl sulfate–piperidine marker specific for guanine. (b) Differential cleavage plot for the difference in susceptibility of *pTyr2* DNA to DNase I digestion in the presence of 2.5 μM nogalamycin. Presentation as described in the legend to Figure 3.

guanine-specific reaction with methylene blue. It has previously been shown that nogalamycin inhibits the reaction of dimethyl sulfate with N7 of guanine (in the double-helical major groove) at positions 22, 45, 69, 117, and 132 in the *tyr*T DNA fragment (Fox & Howarth, 1985). By contrast, actinomycin D, which binds to the dinucleotide step GpC from the minor groove, had little or no effect on the dimethyl sulfate reaction. Figure 6 depicts the products of the methylene blue G specific reaction in the presence of various antibiotics. It is immediately apparent that actinomycin D has drastically reduced the intensity of bonds at positions 36, 72, 75, 77, 94, 101, 117, and 132. Each of these represents the step GpC (see Figure 3) to which actinomycin is known to bind, and all are part of actinomycin-induced blockage sites on the *tyrT* fragment (Fox & Waring, 1984b). In contrast, nogalamycin has reduced the intensity of the G bands at positions 62, 69, and 117 and to a lesser extent those at positions 22, 34, 38, 39, 45, 54, and 57. In general, these blockages correspond with antibiotic binding sites as determined by DNase I footprinting, the only exceptions occurring at positions 45 and 62. Possible reasons for these small differences will be considered further under Discussion, along with the differential effects on susceptibility to methylene blue and dimethyl sulfate. In parallel experiments, neither daunomycin, mithramycin, distamycin, spermine, nor ethidium significantly affected the reaction with methylene blue; tracks showing the lack of effect of the first three of these ligands are included at the right-hand side of Figure 6.

Discussion

The results presented in this paper show that nogalamycin does induce considerable changes in the susceptibility of particular nucleotide sequences to attack by DNase I. At low concentrations the antibiotic produces footprinting patterns in which protected regions appear about four or five base pairs long, similar to the binding site size of six to eight nucleotides estimated by biophysical measurements (Das et al., 1974). In this respect it differs markedly from the simpler anthracyclines such as daunomycin. It appears that the unusual structure of nogalamycin, having bulky sugar substituents that must come to lie in both DNA grooves, effectively endows the antibiotic with the ability to discriminate between different nucleotide sequences. What then is the preferred sequence to which this antibiotic binds, and what is the basis for its preference(s)?

Sequence Selectivity. Close inspection of the DNase I footprinting patterns produced by nogalamycin with the four DNA fragments does not reveal that any particular dinucleotide step constitutes a uniquely preferred binding site. At first sight it appears that many of the protected regions contain the dinucleotide step GpT (ApC) or TpG (CpA): for example, positions 58 (GpT), 69–70 (TpGpT), 93 (TpG), and

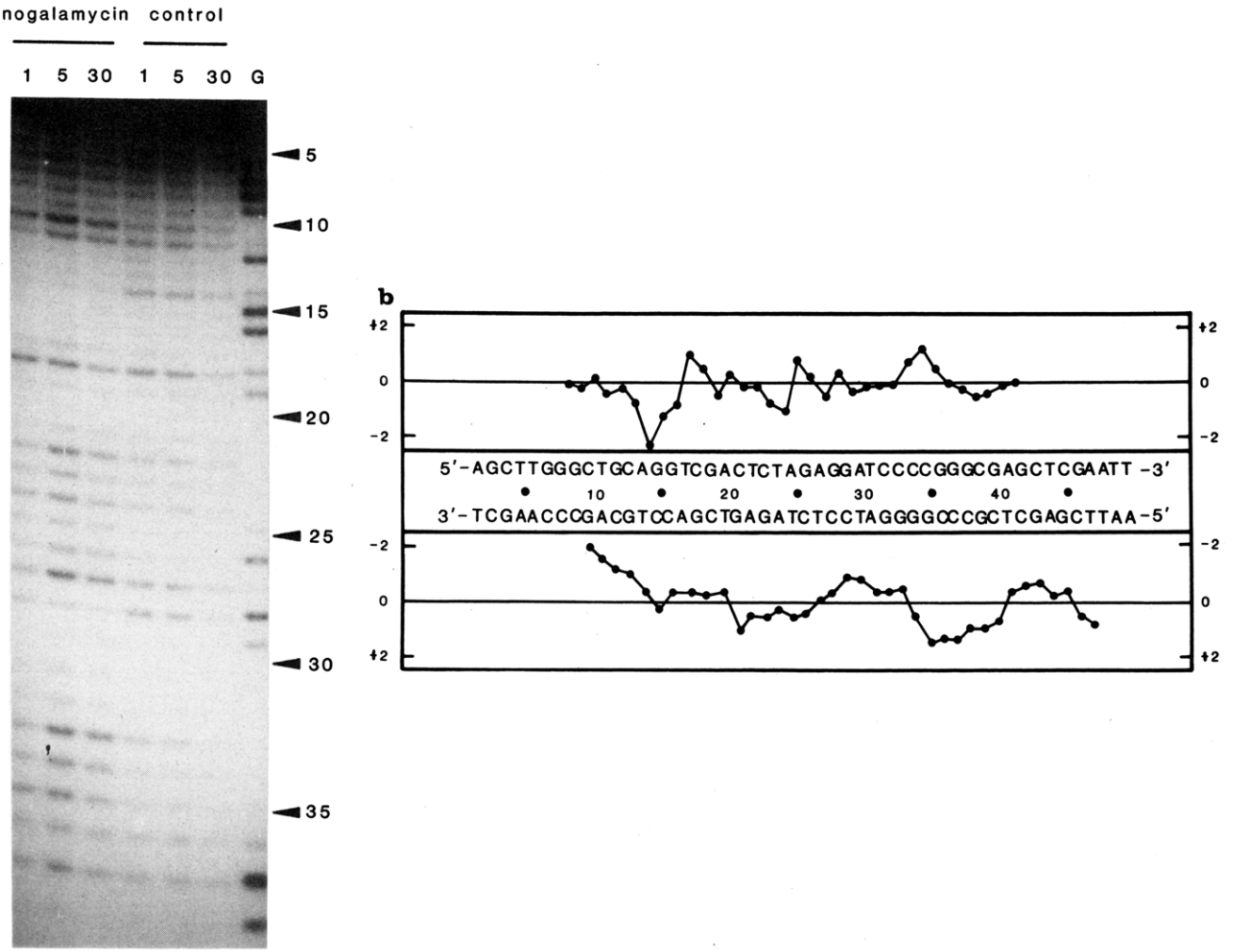

FIGURE 5: (a) DNase I footprinting of nogalamycin (2.5 μM) on the top strand of the *pUC13* multiple-cloning DNA fragment whose sequence is shown in (b). Time in minutes is shown at the top of each gel lane. The track labeled "G" is a dimethyl sulfate–piperidine marker specific for guanine. (b) Differential cleavage plot for the difference in susceptibility of *pUC13* DNA to DNase I digestion in the presence of 2.5 μM nogalamycin. Presentation as described in the legend to Figure 3.

118 (TpG) on the *tyrT* fragment. However, not all such sequences are protected in any of the DNA fragments we have studied, and the apparent correlation may merely indicate that the antibiotic binds best to regions of mixed nucleotide sequence. We are inclined to the view that the footprinting patterns produced by nogalamycin do not simply arise from direct recognition of any particular nucleotide sequence but are primarily determined by the local dynamic properties of the DNA helix. According to this model, the observed binding specificity reflects the ease with which it is possible to distort the local DNA structure in to a form amenable to antibiotic binding. Clearly, this property is unlikely to be constant for all sequences. Drew and Travers (1984) have demonstrated that, for the *tyrT* fragment, the precise local DNA structure is profoundly influenced by the sequence, which in turn alters the susceptibility to nuclease attack. These factors must also influence the ability to bind ligands such as nogalamycin. Many of the antibiotic-protected regions contain runs of alternating pyrimidines and purines at least four nucleotides long. For example, nogalamycin blocks cleavage of the *tyrT* fragment at positions 21, 35, 58, and 69 within the sequences TACG, TACGCA, ACGTA, and TACA, respectively. Could it be that the antibiotic is able to recognize some peculiar dynamic feature of this type of alternating DNA sequence? Unfortunately this cannot be the sole determinant of recognition since in the *tyrT* fragment the alternating sequences ACAC and GCGCGT around positions 63 and 77, respectively, are unaffected. The latter sequence is likely to be relatively stable since Ornstein et al. (1978) have shown that the dinucleotide step GpC is hardest to unstack.

It seems then that nogalamycin binds best to regions of alternating purines and pyrimidines especially those of mixed sequence containing the dinucleotide pairs GpT (ApC) or TpG (CpA). It must however be emphasized that the antibiotic is not excluded from other sites since at higher concentrations the footprinting pattern changes as the antibiotic evidently binds to more sites, with lower affinity.

Mode of Binding. Apart from the thorny question as to which sequences bind nogalamycin best, a further problem concerns the orientation of the ligand when bound to DNA. Model building studies have indicated that it is sterically possible to accommodate either of the two sugar residues in each helical groove (Collier et al., 1984). It is not unlikely that the orientation of the antibiotic will affect the footprinting pattern observed. However, any influences originating from ligand orientation should be less pronounced for DNase I footprinting than for experiments with other simpler cleavage reagents since the blockages arise not only from steric occlusion by the presence of the ligand but also from distortion of the DNA backbone to a form not easily recognized by the enzyme, as a consequence of intercalation-related helical unwinding. According to this reasoning, the chemically simpler G-specific reactions with dimethyl sulfate and methylene blue should be more sensitive to the orientation of the ligand since inhibition

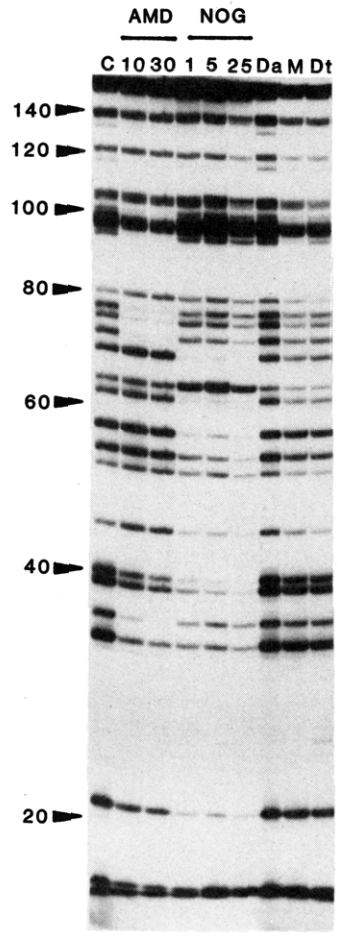

FIGURE 6: Methylene blue photosensitized guanine-specific reaction with *tyrT* DNA labeled at the 3′ end of the bottom strand in the presence of various ligands. C, control; AMD, actinomycin D (10 and 30 μM); NOG, nogalamycin (1, 5, and 25 μM); Da, daunomycin (30 μM); M, mithramycin (30 μM); Dt, distamycin (10 μM).

here is to all intents and purposes a steric effect. Dimethyl sulfate is known to react with N7 of guanine in the major groove and is unaffected by actinomycin D binding in the minor groove (Fox & Howarth, 1985). The mechanism of the reaction with methylene blue is less certain, but it is tempting to speculate that it occurs via the minor groove since it is highly sensitive to protection by actinomycin D. If these two G-specific reagents do indeed modify DNA from opposite grooves, then we may perceive a ready explanation for the differences in blockage produced by nogalamycin. Most likely, the more rigid amino sugar of nogalamycin, carrying a positive charge to stabilize its interaction with DNA, will provide better protection than the more flexible nogalose moiety. If so, we can speculate that the antibiotic is preferentially positioned with its amino sugar in the minor groove at positions 70 and 118 of the *tyrT* fragment, whereas the converse holds true for the other sites. The strong inhibition of the reaction with methylene blue at position 62 remains puzzling since this region is not well protected from cleavage by DNase I.

Structural Changes upon Binding. These results once again demonstrate that a common feature of DNA binding ligands is the ability to induce enhanced rates of cleavage at regions surrounding certain of their binding sites. Enhancement effects of this sort have previously been explained by suggesting that when they occur at AT-rich regions, it is because the neighboring ligand has induced a local widening of the minor groove, restoring it to a more normal "B-DNA-like" structure (Fox & Waring, 1984b; Low et al., 1984a,b). Enhanced susceptibility to DNase I attack as a result of nogalamycin binding is also found in AT-rich regions, notably at positions 30 and 50 on the *tyrT* fragment and at position 65 in *pTyr*2 DNA. While enhanced cleavage at these sites has previously been observed with actinomycin D, echinomycin, and mithramycin (Fox & Waring, 1984b; Low et al., 1984a; Fox & Howarth, 1985), the effects of all ligands are not identical (especially the strong enhancement at positions 80–82 visible on the bottom strand of *tyrT* DNA), and the results serve to emphasize the unusual sequence selectivity of nogalamycin.

Comparison with Daunomycin. The large differences between the footprinting patterns observed with daunomycin and nogalamycin could be due to several factors. First, it might be suggested that daunomycin does not yield a clear pattern of protection because its dissociation from DNA is much faster (Fox et al., 1985). However, this is not a sufficient explanation because lowering the temperature, thereby slowing the dissociation, results in a clearer yet different cleavage pattern for daunomycin (results not shown). Another explanation could be based on the smaller unwinding angle for daunomycin (11°) compared with that of nogalamycin (18°) (Gale et al., 1981). Possibly daunomycin does not cause a large enough perturbation of the DNA structure to produce significant effects on the pattern of cleavage by DNase I. A third, more likely, explanation is that daunomycin has little sequence selectivity while nogalamycin, because of its peculiar structure, has a restricted ability to interact with many DNA sequences.

ACKNOWLEDGMENTS

We thank Drs. H. R. Drew and C. M. L. Low for advice and encouragement.

Registry No. Nogalamycin, 1404-15-5.

REFERENCES

Arcamone, F. (1981) *Doxorubicin. Anticancer Antibiotics*, Academic, New York.

Arora, S. K. (1983) *J. Am. Chem. Soc. 105*, 1328–1332.

Bhuyan, B. K., & Deitz, A. (1965) *Antimicrob. Agents Chemother. 1965*, 836–844.

Bhuyan, B. K. & Smith, C. G. (1965) *Proc. Natl. Acad. Sci. U.S.A. 54*, 566–572.

Bhuyan, B. K., & Reusser, F. (1970) *Cancer Res. 30*, 984–989.

Brown, J. R. (1983) in *Molecular Aspects of Anti-Cancer Drug Action* (Neidle, S., & Waring, M. J. Eds.) pp 57–92, Macmillan, London.

Chowdhury, K., Chowdhury, I., Biswas, N., & Neogy, R. K. (1978) *Indian J. Biochem. Biophys. 15*, 373–376.

Collier, D. A., Neidle, S., & Brown, J. R. (1984) *Biochem. Pharmacol. 33*, 2877–2880.

Das, G. C., Dasgupta, S., & Dasgupta, N. N. (1974) *Biochim. Biophys. Acta 353*, 274–282.

Drew, H. R., & Travers, A. A. (1984) *Cell (Cambridge, Mass.) 37*, 491–501.

Fox, K. R., & Waring, M. J. (1984a) *Biochim. Biophys. Acta 802*, 162–168.

Fox, K. R., & Waring, M. J. (1984b) *Nucleic Acids Res. 12*, 9271–9285.

Fox, K. R., & Howarth, N. R. (1985) *Nucleic Acids Res. 13*, 8695–8714.

Fox, K. R., & Waring, M. J. (1986) *Nucleic Acids Res. 14*, 2001–2014.

Fox, K. R., Brassett, C., & Waring, M. J. (1985) *Biochim. Biophys. Acta 840*, 383–392.

Friedmann, T., & Brown, D. M. (1978) *Nucleic Acids Res. 5*, 615–622.

Gale, E. F., Cundliffe, E., Reynolds, P. E., Richmond, M. H., & Waring, M. J. (1981) in *The Molecular Basis of Antibiotic Action*, 2nd ed., pp 258–401, Wiley, London.
Goodisman, J., & Dabrowiak, J. C. (1985) *J. Biomol. Struct. Dyn. 2*, 967–979.
Ihn, W., Schlegel, B., Fleck, W. F., & Sedmera, P. (1980) *J. Antibiot. 33*, 1457–1461.
Kersten, W., Kersten, H., & Szybalski, W. (1966) *Biochemistry 5*, 236–244.
Lane, M. J., Dabrowiak, J. C., & Vournakis, J. N. (1983) *Nucleic Acids Res. 12*, 4865–4879.
Low, C. M. L., Drew, H. R., & Waring, M. J. (1984a) *Nucleic Acids Res. 12*, 4865–4879.
Low, C. M. L., Olsen, R. K., & Waring, M. J. (1984b) *FEBS Lett. 176*, 414–420.
Ornstein, R. L., Rein, R., Breen, D. L., & MacElroy, R. D. (1978) *Biopolymers 17*, 2341–2360.
Peterson, R. C., Doering, J. L., & Brown, D. D. (1980) *Cell (Cambridge, Mass.) 20*, 4445–4467.
Plumbridge, R. W., & Brown, J. R. (1979) *Biochem. Pharmacol. 28*, 3231–3234.
Van Dyke, M. W., & Dervan, P. B. (1983) *Biochemistry 22*, 2373–2377.
Van Dyke, M. W., Hertzberg, R. P., & Dervan, P. B. (1982) *Proc. Natl. Acad. Sci. U.S.A. 79*, 5470–5474.
Waring, M. J. (1970) *J. Mol. Biol. 54*, 247–279.

Isolation of a Multifunctional Protein with Aminoimidazole Ribonucleotide Synthetase, Glycinamide Ribonucleotide Synthetase, and Glycinamide Ribonucleotide Transformylase Activities: Characterization of Aminoimidazole Ribonucleotide Synthetase†

J. L. Schrimsher, F. J. Schendel, and J. Stubbe*,‡
Department of Biochemistry, College of Agricultural and Life Sciences, University of Wisconsin—Madison, Madison, Wisconsin 53706

Received December 11, 1985; Revised Manuscript Received February 19, 1986

ABSTRACT: 5-Aminoimidazole ribonucleotide (AIR) synthetase, glycinamide ribonucleotide (GAR) synthetase, and GAR transformylase activities from chicken liver exist on a single polypeptide of M_r 110000 [Daubner, C. S., Schrimsher, J. L., Schendel, F. J., Young, M., Henikoff, S., Patterson, D., Stubbe, J., & Benkovic, S. J. (1985) *Biochemistry 24*, 7059–7062]. Details of copurification of these three activities through four chromatographic steps are reported. The ratios of these activities remain constant throughout the purification. AIR synthetase has an absolute requirement for K^+ for activity and under these conditions has apparent molecular weights of 330000, determined by Sephadex G-200 chromatography, and 133000, determined by sucrose density gradient ultracentrifugation. Incubation of ^{18}O-labeled formylglycinamidine ribonucleotide (FGAM) with AIR synthetase results in stoichiometric production of AIR, ADP, and [^{18}O]P_i. NMR spectra of β-FGAM and β-AIR are reported.

In 1963, French and Buchanan (Flaks & Lukens, 1963) reported a 10-fold purification and characterization of aminoimidazole ribonucleotide synthetase from pigeon liver. This enzyme catalyzes the conversion of formylglycinamidine ribonucleotide (FGAM)[1] and ATP to aminoimidazole ribonucleotide (AIR), ADP, and P_i (eq 1). Since this early study,

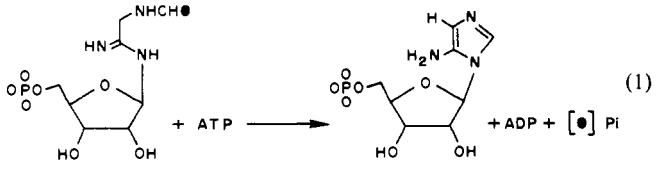

(1)

no further progress has been reported toward isolation and purification of this fifth enzyme in the purine biosynthetic pathway. This is due in part to the difficulty in preparation of the substrate FGAM and in part to the reported instability of protein (Flaks & Lukens, 1963).

The recent results of an investigation between our laboratory and laboratories of Benkovic, Patterson, and Henikoff have established that AIR synthetase is part of a multifunctional protein which also contains two other activities of enzymes involved in purine biosynthesis, namely, glycinamide ribonucleotide (GAR) synthetase and glycinamide ribonucleotide transformylase (Daubner et al., 1985).

While GAR synthetase has not been previously isolated from chicken liver, GAR transformylase has been recently purified from this source by Caperelli et al. (1980) and more efficiently by Young et al. (1984) using a 10-formyl-5,8-dideazafolate affinity column. Thus, unknowingly, the isolation of GAR transformylase by Benkovic and his collaborators also con-

†This research was supported by Grant GM 32191 from the U.S. Public Health Service.
* Correspondence should be addressed to this author.
‡Recipient of an H. I. Romnes Award from the University of Wisconsin and Research Career Development Award AM 01222.

[1] Abbreviations: AIR, 5-aminoimidazole ribonucleotide; FGAM, formylglycinamidine ribonucleotide; PMSF, phenylmethanesulfonyl fluoride; AIRs, 5-aminoimidazole ribonucleoside; GAR, glycinamide ribonucleotide; Tris, tris(hydroxymethyl)aminomethane; FGAR, formylglycinamide ribonucleotide; HEPES, *N*-(2-hydroxyethyl)piperazine-*N*′-2-ethanesulfonic acid; TEAB, triethylammonium bicarbonate; AICAR, 5-aminoimidazolecarboxamide ribonucleotide; ATPγS, adenosine 5′-*O*-(3-thiotriphosphate); EDTA, ethylenediaminetetraacetic acid; SDS, sodium dodecyl sulfate; Me_2SO, dimethyl sulfoxide; Cl_3CCOOH, trichloroacetic acid; FID, free induction decay.

0006-2960/86/0425-4356$01.50/0